

# TRILEPTONS FROM CHARGINO-NEUTRALINO PRODUCTION AT THE CERN LARGE HADRON COLLIDER

Howard Baer<sup>1</sup>, Chih-hao Chen<sup>1</sup>, Frank Paige<sup>2</sup>  
and Xerxes Tata<sup>3</sup>

<sup>1</sup>*Department of Physics, Florida State University, Tallahassee, FL 32306 USA*

<sup>2</sup>*Brookhaven National Laboratory, Upton, NY 11973 USA*

<sup>3</sup>*Department of Physics and Astronomy, University of Hawaii, Honolulu, HI 96822 USA*  
(August 12, 2018)

## Abstract

We study direct production of charginos and neutralinos at the CERN Large Hadron Collider. We simulate all channels of chargino and neutralino production using ISAJET 7.07. The best mode for observing such processes appears to be  $pp \rightarrow \tilde{W}_1 \tilde{Z}_2 \rightarrow 3\ell + \cancel{E}_T$ . We evaluate signal expectations and background levels, and suggest cuts to optimize the signal. The trilepton mode should be viable provided  $m_{\tilde{g}} \lesssim 500 - 600$  GeV; above this mass, the decay modes  $\tilde{Z}_2 \rightarrow \tilde{Z}_1 Z$  and  $\tilde{Z}_2 \rightarrow H_\ell \tilde{Z}_1$  become dominant, spoiling the signal. In the first case, the leptonic branching fraction for  $Z$  decay is small and additional background from  $WZ$  is present, while in the second case, the trilepton signal is essentially absent. For smaller values of  $m_{\tilde{g}}$ , the trilepton signal should be visible above background, especially if  $|\mu| \simeq m_{\tilde{g}}$  and  $m_{\tilde{\ell}} \ll m_{\tilde{g}}$ , in which case the leptonic decays of  $\tilde{Z}_2$  are enhanced. Distributions in dilepton mass  $m(\ell\bar{\ell})$  can yield direct information on neutralino masses due to the distribution cutoff at  $m_{\tilde{Z}_2} - m_{\tilde{Z}_1}$ . Other distributions that may lead to an additional constraint amongst the chargino and neutralino masses are also examined.

## I. INTRODUCTION

The search for supersymmetric (SUSY) particles is one of the major issues in particle physics today [1]. Direct searches for SUSY particles at the LEP  $e^+e^-$  collider have led to mass bounds [2],

$$m_{\tilde{q}}, m_{\tilde{W}_1}, m_{\tilde{\ell}} \gtrsim 40-45 \text{ GeV}, \quad (1)$$

where prospects for higher mass searches are linked to increases in beam energy. At hadron colliders, most searches have focussed on gluino and squark production; here, the CDF and D0 experiments have obtained mass limits of [3,4]

$$m_{\tilde{q}}, m_{\tilde{g}} \gtrsim 100-150 \text{ GeV}, \quad (2)$$

based on non-observation of events with missing transverse energy ( $\cancel{E}_T$ ) plus jets above expected background levels.

Recently, much attention has focussed on the clean trilepton signal from  $p\bar{p} \rightarrow \tilde{W}_1 \tilde{Z}_2 X$ , where  $\tilde{W}_1 \rightarrow \ell \nu \tilde{Z}_1$  and  $\tilde{Z}_2 \rightarrow \ell \bar{\ell} \tilde{Z}_1$ . One expects events containing three hard, isolated leptons plus  $\cancel{E}_T$  with jet activity only from QCD radiation; standard model (SM) backgrounds are expected to be tiny. The importance of this signature has been pointed out long ago for *on shell*  $W$  decays [5]; it was then pointed out that the total  $\tilde{W}_1 \tilde{Z}_2$  cross section remains substantial even for *off-shell*  $W$  decays [6], so that the trilepton signal may be observable with an accumulated data sample of  $\sim 100 \text{ pb}^{-1}$ . Subsequently, it was shown that there could be a large enhancement of the trilepton signal [7], especially when  $m_{\tilde{\ell}} \ll m_{\tilde{q}}$  as is the case in the “no-scale” limit of supergravity (SUGRA) models. In favorable cases, given sufficient luminosity, it may be possible for Tevatron  $p\bar{p}$  collider experiments to probe chargino masses even beyond the reach of LEP 200, corresponding to gluino masses in the several hundred GeV region. This has since been confirmed by calculations of the trilepton rate within the no-scale flipped  $SU(5) \times U(1)$  supergravity framework [8]. Detailed simulation of the trilepton signal and background have been carried out in Ref. [9], where the importance of the dilepton invariant mass distribution was stressed for obtaining a measurement of  $m_{\tilde{Z}_2} - m_{\tilde{Z}_1}$ . Very recently, the CDF [10] and D0 [4] collaborations have reported preliminary bounds on  $m_{\tilde{W}_1}$  from a non-observation of trilepton events in their analysis of  $\sim 10 \text{ pb}^{-1}$  of their data. Although these analyses do not (yet) significantly improve on the bounds from LEP, they clearly establish the viability of this signature.

The higher energy ( $\sqrt{s} = 14 \text{ TeV}$ ) and higher luminosity ( $10^{33}-10^{34} \text{ cm}^{-2}\text{s}^{-1}$ ) anticipated for the CERN Large Hadron Collider (LHC) project should substantially increase the range of parameter space to be probed via the clean trilepton signal. This was first examined in Ref. [11], and later in greater detail, by Barbieri *et. al.* [12]. These authors [12] warned that at the LHC the SM background from  $t\bar{t}$  production — largely negligible at Tevatron energies — may remain problematic (owing to the large top pair total cross section), especially if  $m_t$  was around 120–130 GeV. For example, in going from Tevatron to LHC colliders, the  $\tilde{W}_1 \tilde{Z}_2$  production cross section increases by a factor of  $\sim 10$ , while total  $t\bar{t}$  background cross section ( $m_t = 175 \text{ GeV}$ ) increases by a factor of  $\sim 160$ . In their study, however, they had assumed that the branching fractions for neutralinos were the same as those of the  $Z$  boson which, as we have mentioned, often leads to an underestimate of the signal. On the other

hand, when probing higher mass scales associated with the LHC, possible new chargino and neutralino decay modes may open up, leading to loss of signal. It is also possible that other chargino and neutralino reactions, *e.g.*  $\tilde{W}_1\tilde{Z}_3$  production, become accessible at the larger LHC energy and also contribute to the signal. Finally, if  $\tilde{W}_1\tilde{Z}_2$  events can be isolated from other sources of trileptons, the high event rate expected may allow for substantial precision in the  $m_{\tilde{Z}_2} - m_{\tilde{Z}_1}$  mass measurement, assuming a signal is found.

In this paper, we seek to answer the following questions:

1. Can one find a set of cuts to allow a signal to be claimed above SM backgrounds?
2. If so, in what regions of parameter space is a signal likely observable?
3. Is it possible to separate the trilepton signal from direct chargino-neutralino production from the same signal coming from the cascade decays of gluinos and squarks?
4. Can one gain information on the chargino and neutralino masses?

To answer these, we perform detailed simulations of signal and background using ISAJET 7.07 [13]. In Sec. II, we present an overview of total production cross sections, relevant branching fractions, and details of our simulation. In Sec. III, we try to find an optimal set of cuts to enhance signal over background, and we outline the regions of parameter space where a detectable signal can be expected at the LHC. We study strategies for extracting information about chargino and neutralino masses in Sec. IV. We show that for regions of parameters where  $\tilde{Z}_2 \rightarrow \tilde{Z}_1 H_\ell$  or  $\tilde{Z}_2 \rightarrow \tilde{Z}_1 Z$  decays are kinematically inaccessible, it should be possible to obtain  $m_{\tilde{Z}_2} - m_{\tilde{Z}_1}$  with reasonable precision. We also discuss the possibility of other mass measurements. We conclude in Sec. V with discussion of our results.

## II. CHARGINO AND NEUTRALINO PRODUCTION, DECAY AND EVENT SIMULATION

We work within the framework of the Minimal Supersymmetric Model (MSSM) [1], which is the simplest supersymmetric extension of the SM. Our MSSM mass and parameter choices are inspired, but not ruled by, supergravity models with electroweak symmetry breaking: in particular, we take the higgsino mass parameter  $\mu$  as a free parameter, although it usually scales with  $m_{\tilde{g}}$ , in SUGRA models [14,15] with radiative breaking of electroweak symmetry. In minimal supergravity models, supersymmetry breaking leads to a common mass for sfermions at the unification scale. The degeneracy of sfermions present at the unification scale is broken when these masses are evolved down to the weak scale. We therefore assume slepton masses are related to  $m_{\tilde{q}}$ ,  $m_{\tilde{g}}$  and  $\tan\beta$  as given by the renormalization group equation (RGE) solutions listed in Ref. [7]. Thus, for  $m_{\tilde{q}} \gg m_{\tilde{g}}$ , the squarks are basically degenerate with the sleptons; significant splitting between the masses of the sleptons and squarks is possible only when squarks and gluinos are roughly degenerate, in which case sleptons are considerably lighter than squarks: this latter situation is frequently realized in “no-scale” models [16], in which neutralino decays to leptons can be enhanced [7,8]. However, the trilepton signal may be considerably reduced when decays  $\tilde{W}_1 \rightarrow \ell\tilde{\nu}$  or  $\tilde{Z}_2 \rightarrow \tilde{\ell}_R\bar{\ell} + \tilde{\ell}_R\ell$  because the daughter lepton tends to be soft, reducing the efficiency for passing cuts.

Pair production of charginos and neutralinos at hadron colliders takes place via  $pp \rightarrow \widetilde{W}_i \widetilde{Z}_j X$  (eight reactions),  $pp \rightarrow \widetilde{W}_i \widetilde{W}_j X$  (three reactions), and  $pp \rightarrow \widetilde{Z}_i \widetilde{Z}_j X$  (ten reactions). In Fig. 1, we illustrate total pair production cross sections at  $\sqrt{s} = 14$  TeV (LHC energy) for  $\widetilde{W}_1 \widetilde{Z}_1$ ,  $\widetilde{W}_1 \widetilde{Z}_2$ ,  $\widetilde{W}_1 \widetilde{W}_1$ , and  $\widetilde{Z}_2 \widetilde{Z}_2$  production. We have convoluted with EHLQ Set 1 parton distributions [17]. We show curves versus  $m_{\widetilde{g}}$  for  $(m_{\widetilde{q}}/m_{\widetilde{g}}, \tan \beta) = (1,2)$  (solid),  $(1,20)$  (dashed) and  $(2,2)$  (dotted), and have taken  $\mu = -m_{\widetilde{g}}$  throughout. For  $m_{\widetilde{g}}$  on the low end of the scale, cross sections can be very large due to production via *on-shell*  $W$  and  $Z$  decays. For larger values of  $m_{\widetilde{g}}$ , the chargino and neutralino masses increase, and the cross sections decrease rapidly because production now takes place via *off-shell*  $W$ ,  $\gamma$  and  $Z$  graphs, as well as squark exchange. Even so, we see that the  $\widetilde{W}_1 \widetilde{W}_1$  and  $\widetilde{W}_1 \widetilde{Z}_2$  cross sections remain above the  $0.1$  pb level, owing to a large gauge coupling, even for  $m_{\widetilde{g}} \sim 1000$  GeV. Other chargino-neutralino production processes occur at typically much lower rates, and hence are less likely to give interesting phenomenology. The most interesting of the chargino-neutralino reactions, as we shall see, is  $\widetilde{W}_1 \widetilde{Z}_2$  production. This production rate is actually highest for large values of  $m_{\widetilde{q}}$ , due to negative interference between squark exchange and  $W^*$  exchange amplitudes.

The branching fractions for two decay modes of the light chargino,  $\widetilde{W}_1$ , are shown versus  $m_{\widetilde{g}}$  in Fig. 2, again for *a*)  $(m_{\widetilde{q}}/m_{\widetilde{g}}, \tan \beta) = (1,2)$ , *b*)  $(1,20)$  and *c*)  $(2,2)$ , with  $\mu = -m_{\widetilde{g}}$ . The dashed curves shows the branching fraction for  $\widetilde{W}_1^+ \rightarrow \mu^+ \nu_\mu \widetilde{Z}_1$ , which typically varies between 10-20%, depending on parameter choices, and is  $\sim 11\%$  for large values of  $m_{\widetilde{q}}$  and  $m_{\widetilde{g}}$ , for which decay via virtual  $W$  dominates. For small values of  $m_{\widetilde{g}}$ , the decay  $\widetilde{W}_1 \rightarrow \ell \bar{\nu}$  is kinematically accessible, and is the dominant decay mode. For values of  $m_{\widetilde{g}} > 550$ –600 GeV, two body decays to real  $W$  bosons become kinematically allowed, and dominate the  $\widetilde{W}_1$  branching fractions in this region.

Several decay modes of the neutralino  $\widetilde{Z}_2$  are shown versus  $m_{\widetilde{g}}$  in Fig. 3, for the same cases *a*), *b*) and *c*) as in Fig. 2. The dashed curves shows the branching fraction for  $\widetilde{Z}_2 \rightarrow \mu^+ \mu^- \widetilde{Z}_1$ , which is  $\sim 10 - 20\%$  for  $m_{\widetilde{q}} \sim m_{\widetilde{g}}$ , but only a few per cent for  $m_{\widetilde{q}} \sim 2m_{\widetilde{g}}$ , where decay via a virtual  $Z$  becomes important. Two body modes such as  $\widetilde{Z}_2 \rightarrow \nu \bar{\nu}$  dominate for small  $m_{\widetilde{g}}$ . Just as for the light chargino, other two body decay modes of  $\widetilde{Z}_2$  open up around  $m_{\widetilde{g}} \sim 600$  GeV. In case *a*), the decay  $\widetilde{Z}_2 \rightarrow \widetilde{Z}_1 H_\ell$  dominates, and one expects very few leptons from  $\widetilde{Z}_2$ . In case *b*) and *c*), the mode  $\widetilde{Z}_2 \rightarrow \widetilde{Z}_1 Z$  opens up first, and there is a region in which one expects real  $Z \rightarrow \ell \bar{\ell}$  in the event sample. As we shall see, the opening of these two body  $\widetilde{Z}_2$  modes can effectively spoil the clean trilepton signal from  $\widetilde{W}_1 \widetilde{Z}_2$  production, in one case because the leptonic branching fraction for the  $Z$  is rather small, and additional background from  $WZ$  appears, and in the other because the Higgs boson essentially always decays to  $b$ -quarks.

In order to assess detection prospects for charginos and neutralinos at LHC energy, we use the event simulation program ISAJET 7.07 [13]. For a given input parameter set,  $m_{\widetilde{g}}, m_{\widetilde{q}}, \mu, \tan \beta, m_{H_p}, m_t$  and  $m_{\widetilde{\ell}_L}, m_{\widetilde{\ell}_R}, m_{\widetilde{\nu}_L}$ , (recall that  $m_{\widetilde{\ell}_L}, m_{\widetilde{\ell}_R}, m_{\widetilde{\nu}_L}$  are determined by  $m_{\widetilde{g}}, m_{\widetilde{q}}$  and  $\tan \beta$ ) the routine ISASUSY calculates all sparticle masses and branching fractions to various decay modes. ISAJET then produces all combinations of chargino and neutralino production subprocesses, in proportion to their respective cross sections. The charginos and neutralinos then decay via the various cascades with appropriate branching fractions as given by the MSSM. Radiation of initial and final state partons is also included in ISAJET. Final state quarks and gluons are hadronized, and unstable particles are decayed

until stable final states are reached. Underlying event activity is also modeled in ISAJET.

For event simulation at the LHC, we use the toy calorimeter simulation package ISAPLT. We simulate calorimetry with cell size  $\Delta\eta \times \Delta\phi = 0.05 \times 0.05$ , which extends between  $-5.5 < \eta < 5.5$ . We take hadronic energy resolution to be  $50\%/\sqrt{E_T}$  for  $|\eta| < 3$ , and to be a constant 10% for  $3 < |\eta| < 5.5$ , to model the effective  $p_T$  resolution of the forward calorimeter including the effects of shower spreading. We take electromagnetic resolution to be  $15\%/\sqrt{E_T}$ . Jets are coalesced within cones of  $R = \sqrt{\Delta\eta^2 + \Delta\phi^2} = 0.7$  using the ISAJET routine GETJET. For the purpose of jet veto (essential to eliminate top quark background), clusters with  $E_T > 25$  GeV are labeled as jets. Muons and electrons are classified as isolated if they have  $p_T > 10$  GeV,  $|\eta(\ell)| < 2.5$ , and the visible activity within a cone of  $R = 0.3$  about the lepton direction is less than  $E_T(\text{cone}) = 5$  GeV.

### III. SIGNAL AND BACKGROUND

In our simulation of chargino and neutralino events, we generate all twenty-one of the reactions referred to in Sec. II. We first classify signals according to the number of isolated leptons present in the signal events. We found observable signal cross sections in the  $0\ell$ ,  $1\ell$ ,  $2\ell$  and  $3\ell$  channels. However, the  $0\ell + \text{jets} + \cancel{E}_T$  sample should be dominated by other sources of SUSY events, such as gluino and squark production, as well as SM backgrounds. The  $1\ell + \text{jets} + \cancel{E}_T$  channel yielded observable signal rates; however, these were dominated by large SM backgrounds from  $W \rightarrow \ell\nu_\ell$  ( $\ell = e$  or  $\mu$ ),  $W \rightarrow \tau\nu_\tau$  and  $t\bar{t}$  production, as well as single lepton events from gluino and squark production [18]. Likewise, the opposite sign (OS) dilepton ( $2\ell + \text{jets} + \cancel{E}_T$ ) sample, which has a substantial rate due especially to  $\widetilde{W}_1\widetilde{W}_1$  production, suffers large SM backgrounds mainly from  $t\bar{t}$  production as well as other SUSY sources [18]. Same-sign (SS) dilepton events can occur from processes such as  $\widetilde{W}_1\widetilde{Z}_2$  production, where one of the decay leptons is soft or missed through a crack in the detector, but these rates are small compared to SS dilepton production from squarks and gluinos [18,19]. Unlike these events, the  $\widetilde{W}_1\widetilde{Z}_2$  events would usually be free from jet activity. In this paper, we focus on the zero-jet (clean) trilepton signal, which occurs at a substantial rate due to  $\widetilde{W}_1\widetilde{Z}_2$  production, and which, with an appropriate set of cuts, is relatively free of SM backgrounds. There is also a possibility for  $4\ell$  events from sources such as  $\widetilde{Z}_2\widetilde{Z}_2$  production followed by subsequent leptonic decays. These signals have been considered (as backgrounds to Higgs boson decay to neutralino pairs) in Ref. [20]; cross sections range up to a few fb after cuts, so the signal is not large, although SM physics backgrounds can be eliminated. In addition,  $5\ell$  signals have been considered in Ref. [12]; we did not find significant rates for signal in this channel.

To assess the viability of the trilepton signal at LHC energy, we use ISAJET 7.07 to generate  $\sim 100K$  events for the following four cases, where  $m_{\tilde{q}} = m_{\tilde{g}} + 20$  GeV, and  $\tan\beta = 2$ :

Case 1:  $m_{\tilde{g}} = -\mu = 300$  GeV,  $m_{\widetilde{W}_1} = 95.8$  GeV,  $m_{\widetilde{Z}_2} = 96.4$  GeV,  $m_{\widetilde{Z}_1} = 45$  GeV,

Case 2:  $m_{\tilde{g}} = -\mu = 400$  GeV,  $m_{\widetilde{W}_1} = 123.5$  GeV,  $m_{\widetilde{Z}_2} = 123.8$  GeV,  $m_{\widetilde{Z}_1} = 59.8$  GeV,

Case 3:  $m_{\tilde{g}} = -\mu = 500$  GeV,  $m_{\widetilde{W}_1} = 152.6$  GeV,  $m_{\widetilde{Z}_2} = 152.8$  GeV,  $m_{\widetilde{Z}_1} = 74.8$  GeV,

Case 4:  $m_{\tilde{g}} = -\mu = 600$  GeV,  $m_{\widetilde{W}_1} = 182.7$  GeV,  $m_{\widetilde{Z}_2} = 182.8$  GeV,  $m_{\widetilde{Z}_1} = 90.0$  GeV.

The above parameters are motivated by predictions from supergravity GUT models with radiative electroweak symmetry breaking [14,15]. We also generate SM background event samples from  $WZ$  production, as well as from  $t\bar{t}$  production for  $m_t = 135$  GeV and 175 GeV. Finally, we generate samples with all other possible SUSY particle production processes, to see if the  $\tilde{W}_1\tilde{Z}_2$  component can be isolated.

We first select events by requiring

- *three* isolated leptons; the two fastest have  $p_T(\ell_1, \ell_2) > 20$  GeV, while the third has  $p_T(\ell_3) > 10$  GeV.

The signal cross section before and after cuts for the above four cases, SM backgrounds, and trilepton cross sections from other SUSY sources, are listed in Table 1. At this point, the signal can still be dominated by SM background, but even more so by trilepton events from gluino and squark production. Gluino and squark events should contain substantial jet activity as well as a hard  $\cancel{E}_T$  spectrum. We illustrate the latter for cases 1-3 in Fig. 4: the  $\cancel{E}_T$  spectrum is clearly harder for  $\tilde{g}$  and  $\tilde{q}$  events. Hence, we require in addition

- no central jets, ( $p_T(\text{jet}) > 25$  GeV;  $|\eta(\text{jet})| < 3$ ), and
- $\cancel{E}_T < 100$  GeV.

Contributions to the trilepton signal from  $\tilde{g}$  and  $\tilde{q}$  production are now smaller than the chargino-neutralino signal. At this point, the dominant background is from  $WZ \rightarrow 3\ell$  production, so we require

- for OS same flavor dileptons,  $m(\ell\bar{\ell}) \neq M_Z \pm 8$  GeV.

This reduces the  $WZ$  background to below the  $fb$  level, but leaves a significant  $t\bar{t}$  background, especially for the  $m_t = 135$  GeV case [12]. The latter background can be further reduced by splitting the event sample in two. In the first, we require:

- the two fastest leptons be same sign (SS); and the flavor of the slow lepton be the same as (but anti-) the flavor of either of the two fast leptons.

This diminishes the signal by a factor of about 2, but almost completely removes top quark background, from which the two hardest leptons, almost always, come from the primary decays of the  $t$ -quarks, and hence have opposite signs. Some of the rejected signal can be recovered by also accepting events with:

- two fastest leptons of opposite sign (OS) if  $p_T(\text{slow lepton}) > 20$  GeV,

which is more effective in reducing top quark background than signal.

The sum of these two classes of cuts are listed in the last row of Table I, where we find signal in the 13–40  $fb$  range, with SM background at the level of 0.5–3  $fb$ , depending on  $m_t$ . In addition, there exists an irremovable contribution, shown in parenthesis, from other SUSY sources. We investigated this remaining SUSY background, and found it to be all either associated production events (*e.g.*  $\tilde{g}\tilde{Z}_2$ , etc.) or slepton pair events: the gluino and squark pairs had been completely eliminated. For case 4, the spoiler mode  $\tilde{Z}_2 \rightarrow \tilde{Z}_1 H_\ell$  has opened up, thus destroying the trilepton signal.

In Table II, we list the signal cross sections after all the above cuts as a matrix in  $m_{\tilde{g}}$  vs.  $\mu$  for  $\tan\beta = 2$ . Starred entries are in the LEP excluded region. We see that signal cross sections are usually larger for negative  $\mu$  than for positive  $\mu$ , due mainly to a larger  $\tilde{Z}_2 \rightarrow \tilde{Z}_1 \ell \bar{\ell}$  branching ratio [7]. Also, for negative  $\mu$ , the signal is killed much beyond  $m_{\tilde{g}} = 500$  GeV, while for positive  $\mu$  one gets a robust signal past  $m_{\tilde{g}} = 600$  GeV, especially for the supergravity favored choice,  $\mu = m_{\tilde{g}}$ . For  $\mu = \pm 100$  GeV, a signal of a few  $fb$  persists out to  $m_{\tilde{g}} \sim 700$ – $900$  GeV. In fact, for this region of parameter space, most of the trileptons come from subprocesses other than  $\tilde{W}_1 \tilde{Z}_2$ , with *e.g.*  $\tilde{W}_1 \tilde{Z}_3$ ,  $\tilde{W}_2 \tilde{Z}_4$ , etc., also contributing.

How does the signal depend on other choices of  $m_{\tilde{q}}$  and  $\tan\beta$ ? We show in Fig. 5 data points for signal rates for  $\mu = \pm m_{\tilde{g}}$ , for *a)* the case already considered,  $(m_{\tilde{q}}/m_{\tilde{g}}, \tan\beta) = (1, 2)$ , and also *b)* (2,2), *c)* (1,20) and finally *d)* (2,20). SM background level is indicated by the dotted line, for the worst case with  $m_t = 135$  GeV, and the dashed line for  $m_t = 175$  GeV. We see that frames *a)* and *c)*, with  $m_{\tilde{q}} \sim m_{\tilde{g}}$  so that  $m_{\tilde{\ell}} \ll m_{\tilde{q}}$ , yield the largest signal cross sections, and these signals remain substantially above background out to  $m_{\tilde{g}} \sim 500$ – $600$  GeV. Overall behavior is similar for both large and small values of  $\tan\beta$ . For frames *b)* and *d)*, with  $m_{\tilde{q}} = 2m_{\tilde{g}}$  so that sleptons are quite heavy, signal rates drop to the several  $fb$  level, which may be observable above background for the case of a heavier top quark.

As can be seen in Fig. 3, the two body decay  $\tilde{Z}_2 \rightarrow \tilde{Z}_1 Z$  opens up and is dominant for frame *b)* and *c)* for  $m_{\tilde{g}} \sim 600$ – $800$  GeV. In this case, our cut of  $m(\ell\bar{\ell}) \neq M_Z \pm 8$  GeV will also eliminate the signal. To see if this signal can still be gleaned from background, we implement all the above cuts except the offending  $Z$  mass cut. We set  $m_{\tilde{g}} = 700$  GeV, and take  $m_{\tilde{q}} = 2m_{\tilde{g}}$ , with  $\tan\beta = 2$ . The trilepton cross section is then at the  $3.1 fb$  level, while  $WZ$  background is  $59 fb$ . We attempt to remove the  $WZ$  background by requiring transverse mass  $m_T(\ell, \cancel{E}_T) > 100$  GeV, to exclude the real  $W$  Jacobian peak. This reduces both signal (which is already small on account of the rather large  $\tilde{W}_1$  and  $\tilde{Z}_2$  masses) and background to the  $1 fb$  level, making distinction of this tiny signal very difficult. Hence, the  $\tilde{Z}_2 \rightarrow \tilde{Z}_1 Z$  two body decay also acts as a spoiler mode for trilepton events, in part because the signal becomes rate-limited due to the small leptonic branching ratio of the  $Z$  boson together with the fact that the real  $Z$  mode is open only when the  $\tilde{Z}_2$  (and  $\tilde{W}_1$ ) is rather heavy, but also due to irremovable  $WZ$  background.

In addition, we have investigated whether the  $\tilde{W}_1 \tilde{Z}_2$  signal with  $\tilde{W}_1 \rightarrow \tilde{Z}_1 W$  ( $W \rightarrow \ell\nu$ ) and  $\tilde{Z}_2 \rightarrow \tilde{Z}_1 H_\ell$  ( $H_\ell \rightarrow b\bar{b}$ ) is observable. Here, we looked for a single lepton plus two central jet signal. In addition, we required one  $b$ -jet to have its decay vertex tagged with an efficiency as given in Ref. [9]. We then looked for a mass bump at  $m_{jj} = m_{H_\ell}$ . The mass bump was unfortunately obscured by a  $t\bar{t}$  background  $\sim 100$  times greater than signal. Hence, we affirm that the  $\tilde{Z}_2 \rightarrow \tilde{Z}_1 H_\ell$  decay mode is indeed a spoiler.

#### IV. CONSTRAINING CHARGINO AND NEUTRALINO MASSES

For the values of parameters examined in this paper, there will be a plethora of various signals from SUSY at the LHC just from gluino and squark production [18,19]. The unique feature of the trilepton signal for LHC is that it offers the possibility of reasonably clean information on sparticle masses from which to start to unravel the whole SUSY particle spectrum. With a relatively pure sample of signal events, and an event structure consisting of only three isolated leptons plus no jets, it is especially easy to reconstruct where each

lepton came from: in  $\ell\ell'\bar{\ell}'$  events, the  $\ell'\bar{\ell}'$  come from the neutralino, whereas in  $\ell\ell\bar{\ell}$  events, the OS dilepton with smallest transverse opening angle usually comes from the neutralino.

We show in Fig. 6 the invariant mass  $m(\ell\bar{\ell})$  in trilepton events after all cuts, for cases 1, 2 and 3 above. We show the SM background (dots) and the SUSY signal plus SM and SUSY background (solid), where we have taken the mass of the same flavor OS dilepton pair in  $\ell\ell'\bar{\ell}'$  events, and the mass of the OS pair with the smaller transverse opening angle in  $\ell\ell\bar{\ell}$  events. Kinematically, the mass spectrum is constrained to lie between  $0 < m(\ell\bar{\ell}) < m_{\tilde{Z}_2} - m_{\tilde{Z}_1}$ . The sharp cutoff at the upper end-point is evident from these plots, offering a clean measure of  $m_{\tilde{Z}_2} - m_{\tilde{Z}_1}$ . The corresponding value of  $m_{\tilde{Z}_2} - m_{\tilde{Z}_1}$  in these figures is 51, 64 and 78 GeV, for cases 1, 2 and 3, respectively. In models with  $|\mu|$  much larger than the electroweak gaugino masses (as is the case in SUGRA models), one frequently expects  $2m_{\tilde{Z}_1} \simeq m_{\tilde{Z}_2} \simeq m_{\tilde{W}_1} \simeq \frac{1}{3}m_{\tilde{g}}$  [1], so that the cutoff in  $m(\ell\bar{\ell})$  occurs at approximately  $m_{\tilde{Z}_1}$ : this is true in our simulations.

Are there other distributions which can yield significant information constraining sparticle masses? Explicit mass reconstruction is, of course, not possible since in each event one is missing a neutrino and the two massive  $\tilde{Z}_1$  particles. However, we examined a variety of distributions, including trilepton invariant mass,  $m(3\ell)$ , the summed scalar transverse energy,  $\Sigma E_T = p_T(\ell_1) + p_T(\ell_2) + p_T(\ell_3) + \cancel{E}_T$ , and the three lepton plus missing energy cluster transverse mass,  $m_T(3\ell, \cancel{E}_T)$ . All these distributions suffered substantial smearing due mainly to the continuum nature of the underlying  $2 \rightarrow 2$  subprocess; additional smearing is expected for distributions involving  $\cancel{E}_T$  if LHC is run at high luminosity, where event pile-up becomes a problem. The distributions do scale with overall sparticle mass values. An example is given in Fig. 7 for the cluster transverse mass. The solid histograms show the  $m_T(3\ell, \cancel{E}_T)$  distribution for cases 1, 2 and 3, after all cuts. The distribution maxima increases with increasing sparticle mass, as does the distribution mean, which is 154, 175 and 195 GeV for the respective cases. The distributions are also sensitive to the  $\tilde{Z}_1$  mass, in that if  $m_{\tilde{Z}_1} \rightarrow 0$ , there is more energy available to make visible decay products. To illustrate this, we show via dashed histograms the distribution shapes where we have by hand set the  $\tilde{Z}_1$  mass to zero without changing other masses and branching fractions. In this case, the distribution maxima move substantially to higher energy, and the means move to 195, 225 and 271 GeV, respectively. If a trilepton signal is found above expected background levels, then the shapes of distributions such as cluster transverse mass or summed scalar  $E_T$  will also serve to constrain the sparticle masses. For example, for the plots in Fig. 7, the distribution means can be parameterized as

$$\langle m_T(3\ell, \cancel{E}_T) \rangle = 0.69 \times (m_{\tilde{W}_1} + m_{\tilde{Z}_2}) - 0.95 \times m_{\tilde{Z}_1} + 60 \text{ GeV}. \quad (3)$$

For the various cases in Fig. 7, this reproduces the distribution means to within 3-6 GeV. We have also checked that this is an adequate fit for cases where just the chargino mass is reduced by 20 GeV. It should, however, be remembered that the fit in Eq. (3) is sensitive to the details of the cuts and detector simulation. Our purpose in showing this is to illustrate that it should be possible to obtain further information on the sparticle masses from the transverse mass, summed scalar  $E_T$ , and trilepton invariant mass distributions.

In addition, we have investigated a variety of other distributions which show sensitivity to sparticle masses. In  $\ell'\ell\bar{\ell}$  events, the transverse opening angle  $\Delta\phi(\ell\bar{\ell})$  decreases with increasing  $\frac{m_{\tilde{Z}_2}}{m_{\tilde{Z}_1}}$ , for fixed  $m_{\tilde{Z}_2} - m_{\tilde{Z}_1}$ : *i.e.* the dilepton pair becomes more tightly collimated.



Also, the opening angle  $\Delta\phi(\ell', \ell\bar{\ell})$  (between  $\ell'$  and the vector sum of  $\ell$  and  $\bar{\ell}$ ) increases with increasing  $\frac{m_{\tilde{W}_1}}{m_{\tilde{Z}_1}}$  (again, for fixed  $m_{\tilde{Z}_2} - m_{\tilde{Z}_1}$ ), so that events are more nearly back-to-back. Moreover, the  $p_T(\ell')$  distribution is sensitive to  $m_{\tilde{W}_1}$ . Clearly, if a signal is observed, a variety of distributions will have to be tested against various sparticle mass hypotheses. Likelihood functions can then be constructed to ascertain the most probable sparticle mass combination.

## V. SUMMARY

We have reexamined the signal from the production of charginos and neutralinos at the LHC using ISAJET 7.07, incorporating experimental conditions corresponding to a generic LHC detector. As in Ref. [12], we find that the reaction  $p\bar{p} \rightarrow \tilde{W}_1\tilde{Z}_2 \rightarrow \ell\bar{\ell}\ell'$  provides the best prospects for the identification of the signal. The signal thus consists of events with three hard, isolated leptons and essentially no jet activity. We have devised a set of cuts to reduce backgrounds from top quarks and  $WZ$  production to negligible levels *provided* that two body decays of charginos and neutralinos are kinematically inaccessible. The observation of this signal would be direct evidence for neutralino production; this is especially important since the production of (gaugino-like) neutralinos by  $e^+e^-$  collisions is strongly suppressed unless the selectron is also rather light. The effect of the various cuts as well as the signal level for representative choices of parameters is shown in Table I. We also mention that with these cuts, other SUSY sources of trileptons such as squark or gluino pair production, or the production of gluinos and squarks in association with a chargino contribute between just 3–15% to the signal. The relatively clean sample of chargino and neutralino events, as we will see, enables us to obtain experimental constraints on their masses.

We see from Table I that the signal cross section exceeds 10  $fb$  (corresponding to more than 100 events per year even assuming the lower value for the LHC design luminosity) for chargino and neutralino masses up to about 150 GeV, corresponding to  $m_{\tilde{g}} \simeq 500$  GeV. For yet heavier sparticles (case 4 in Table I), the decays  $\tilde{Z}_2 \rightarrow \tilde{Z}_1 H_\ell$ ,  $\tilde{Z}_2 \rightarrow \tilde{Z}_1 Z$  become kinematically accessible. These then dominate the decays of  $\tilde{Z}_2$ . In the first case, the trilepton cross section is reduced to an unobservable level since the Higgs boson decays to heavy fermions. In the other case where two leptons come from the decay of a real  $Z$ , there remains a background from  $WZ$  production; although a signal to background ratio of 1:1 is possible after a transverse mass cut, the signal appears to be too small for this strategy to be viable. The dependence of the signal on the superpotential parameter  $\mu$  is shown in Table II, while the variation with  $\tan\beta$  and  $m_{\tilde{g}}$  is illustrated in Fig. 5.

Motivated by the fact that after our cuts we are left with a relatively uncontaminated sample of  $\tilde{W}_1\tilde{Z}_2$  events, we have examined the prospects for measuring chargino and neutralino masses from these events. Since the invariant mass of dileptons from  $\tilde{Z}_2$  decays is kinematically constrained to be smaller than  $m_{\tilde{Z}_2} - m_{\tilde{Z}_1}$ , this mass difference can be inferred from the upper edge of the distribution shown in Fig. 6. Since at least several hundred trilepton events are expected at the LHC with an integrated luminosity of 10-20  $fb^{-1}$ , it should be possible to construct this distribution rather well. Unfortunately, it is not possible to directly reconstruct the masses of the  $\tilde{W}_1$  or  $\tilde{Z}_2$  because two neutralinos and the neutrino are undetected in every event. We have shown, however, that by studying

the shapes of other distributions such as the  $m_T(3\ell, \cancel{E}_T)$ -distribution (see Fig. 7), or the  $\Sigma E_T$ -distribution, whose means may be expected to scale with parent masses as discussed in Sec. IV, it should be possible to obtain one further constraint between  $m_{\tilde{Z}_1}$ ,  $m_{\tilde{Z}_2}$  and  $m_{\tilde{W}_1}$ . Ultimately, matching a variety of observed distributions against different sparticle mass hypotheses should allow the most probable combination of sparticle masses consistent with data to be selected. These experimental constraints may serve as a relatively clean starting point for the procedure of unraveling the whole spectrum of SUSY particle masses. Such information ought to help test the ideas behind supergravity grand unification (for instance, the unification of gaugino masses), and further, to aid in sorting out more complex events from the cascade decays of gluinos and squarks.

### ACKNOWLEDGMENTS

This research was supported in part by the U. S. Department of Energy under contract number DE-FG05-87ER40319, DE-AC02-76CH00016, and DE-AM03-76SF00235. In addition, the work of HB was supported by the TNRLC SSC Fellowship program.

## REFERENCES

- [1] For a review of the minimal model and SUSY phenomenology, see H. P. Nilles, Phys. Rep. **110**, 1 (1984); P. Nath, R. Arnowitt and A. Chamseddine, *Applied N = 1 Supergravity*, ICTP Series in Theoretical Physics, Vol. 1, (World Scientific, 1984); H. Haber and G. Kane, Phys. Rep. **117**, 75 (1985); X. Tata, in *The Standard Model and Beyond*, p. 304, edited by J. E. Kim, World Scientific (1991); V. Barger and R. J. N. Phillips, Wisconsin preprint, MAD/PH/765 (1993).
- [2] D. Decamp *et.al.* (ALEPH Collaboration), Phys. Lett. **B236**, 86 (1990); P. Abreu *et.al.* (DELPHI Collaboration), Phys. Lett. **B247**, 157 (1990); O. Adriani *et.al.* (L3 Collaboration), CERN-PPE-93-31 (1993); M. Akrawy *et.al.* (OPAL Collaboration), Phys. Lett. **B240**, 261 (1990); for a review, see G. Giacomelli and P. Giacomelli, CERN-PPE/93-107 (1993).
- [3] F. Abe *et. al.*, Phys. Rev. Lett. **69**, 3439 (1992).
- [4] See talk by A. White, Aspen Winter Conference on Particle Physics, Aspen, CO (1994).
- [5] H. Baer and X. Tata, Phys. Lett. **155B**, 278 (1985); H. Baer, K. Hagiwara and X. Tata, Phys. Rev. Lett. **57**, 294 (1986) and Phys. Rev. **D35**, 1598 (1987).
- [6] P. Nath and R. Arnowitt, Mod. Phys. Lett. **A2**, 331 (1987).
- [7] H. Baer and X. Tata, Phys. Rev. **D47**, 2739 (1993).
- [8] J. Lopez, D. Nanopoulos, X. Wang and A. Zichichi, Phys. Rev. **D48**, 2062 (1993) and CERN-TH-7107-93 (1993).
- [9] H. Baer, C. Kao and X. Tata, Phys. Rev. **D48**, 5175 (1993).
- [10] F. Abe *et. al.*, FERMILAB-CONF-93-213-E (1993).
- [11] R. Arnowitt, R. M. Barnett, P. Nath and F. Paige, Int. J. Mod. Phys. **A2**, 1113 (1987).
- [12] R. Barbieri, F. Caravaglios, M. Frigeni and M. Mangano, Nucl. Phys. **B367**, 28 (1993).
- [13] F. Paige and S. Protopopescu, in *Supercollider Physics*, p. 41, ed. D. Soper (World Scientific, 1986); H. Baer, F. Paige, S. Protopopescu and X. Tata, in *Proceedings of the Workshop on Physics at Current Accelerators and Supercolliders*, ed. J. Hewett, A. White and D. Zeppenfeld, (Argonne National Laboratory, 1993).
- [14] R. Arnowitt and P. Nath, private communication.
- [15] Some recent analyses of supergravity mass patterns include, G. Ross and R. G. Roberts, Nucl. Phys. **B377**, 571 (1992); R. Arnowitt and P. Nath, Phys. Rev. Lett. **69**, 725 (1992); M. Drees and M. M. Nojiri, Nucl. Phys. **B369**, 54 (1993); S. Kelley *et. al.*, Nucl. Phys. **B398**, 3 (1993); G. Kane, C. Kolda, L. Roszkowski and J. Wells, UM-TH-93-24 (1993); V. Barger, M. Berger and P. Ohmann, MAD/PH/801 (1993).
- [16] A. B. Lahanas and D. V. Nanopoulos, Phys. Rep. **145**, 1 (1987).
- [17] E. Eichten, I. Hinchliffe, K. Lane and C. Quigg, Rev. Mod. Phys. **56**, 759 (1984).
- [18] H. Baer, X. Tata and J. Woodside, Phys. Rev. **D45**, 142 (1992); H. Baer, M. Bisset, X. Tata and J. Woodside, Phys. Rev. **D46**, 303 (1992); H. Baer, M. Drees, C. Kao, M. Nojiri and X. Tata, FSU-HEP-940311 (1994).
- [19] See *e.g.* The Solenoidal Detector Collaboration Technical Design Report; GEM Collaboration, Technical Design Report; Report of the Supersymmetry Working Group in Proceedings of the *Large Hadron Collider Workshop*, Aachen, October 1990, CERN90-10; F. Pauss, *ibid*; H. Baer *et. al.* in *Research Directions for the Decade*, E. Berger, Editor (World Scientific, 1992).
- [20] H. Baer, M. Bisset, C. Kao and X. Tata, FSU-HEP-940204 (1994).

# TABLES

TABLE I. Cross sections (in  $fb$ ) after cuts for chargino-neutralino production at LHC for cases 1–4 listed in Sec. III of the text, along with SM backgrounds. Contributions from other SUSY particles are listed in parenthesis below signal rates. We take  $\mu = -m_{\tilde{g}}$  and  $\tan\beta = 2$ . The notations  $3\ell$ ,  $0j$ ,  $\cancel{E}_T$ , and  $M_Z$  refer to the trilepton, jet veto, missing energy, and  $Z$ -mass veto cuts described in the text. The “ $SS, FL$ ” subsample has the two fastest leptons with the same sign and the third with the opposite flavor; the “ $OS, L20$ ” sample has the two fastest leptons with opposite signs and  $p_T(\text{slow lepton}) > 20$  GeV. Results have summed over  $e$ ’s and  $\mu$ ’s. We do not show other SUSY contributions to case 4 because we do not consider this signal to be observable.

cuts	case 1	case 2	case 3	case 4	$t\bar{t}(135)$	$t\bar{t}(175)$	$WZ$
<i>none</i>	11.1K (1521K)	5.1K (386K)	2.6K (124K)	1.5K	2611K	841K	17K
$3\ell$	151 (17.5K)	95 (4.6K)	51 (1.3K)	1.6	486	98	117
$3\ell, 0j$	73 (15)	42 (3.9)	22 (1.0)	0.6	50	2.5	63
$3\ell, 0j, \cancel{E}_T$	72 (8.4)	40 (2.4)	20 (0.4)	0.6	48	2.1	59
$3\ell, 0j, \cancel{E}_T, M_Z$	67.5 (8.4)	37.4 (2.4)	19 (0.4)	0.4	42	1.9	0.8
$3\ell, 0j, \cancel{E}_T, M_Z$ <i>SS, FL</i>	26 (2.1)	15 (1.8)	7.1 (0.2)	0.3	0.4	< 0.2	0.3
$3\ell, 0j, \cancel{E}_T, M_Z$ <i>OS, L20</i>	15 (3.5)	9.0 (0.3)	6.1 (0.1)	0.1	2.0	< 0.2	0.2
$3\ell, 0j, \cancel{E}_T, M_Z$ <i>SS, FL or OS, L20</i>	41 (5.6)	24 (2.1)	13 (0.3)	0.4	2.4	< 0.2	0.5

TABLE II. Trilepton cross sections in  $fb$  after all cuts for various values of  $m_{\tilde{g}}$  and  $\mu$ . A star indicates a point excluded by LEP. We take  $m_{\tilde{q}} = m_{\tilde{g}} + 20$  GeV, and  $\tan\beta = 2$ . The total SM background is 2.9  $fb$  for  $m_t = 135$  GeV, and < 0.7  $fb$  for  $m_t = 175$  GeV. Cuts are described in the text. Results have summed over  $e$ ’s and  $\mu$ ’s.

$m_{\tilde{g}} \backslash \mu$	$-m_{\tilde{g}}$	-400	-300	-200	-100	100	200	300	400	$m_{\tilde{g}}$
300	41.5	49.6	41.5	25.9	1.7	*	10.1	23.0	20.9	23.0
400	23.7	23.7	18.7	3.9	2.2	*	4.3	10.6	14.7	14.7
500	13.2	8.7	4.3	1.3	1.0	4.1	0.9	1.9	7.3	11.5
600	0.4	0.2	0.1	0.8	1.1	4.6	1.1	0.4	1.8	8.8
700	0.1	0.0	0.1	0.6	1.2	2.7	0.7	0.2	0.8	0.0
900	0.0	0.0	0.0	1.3	0.2	1.9	0.1	0.4	0.0	0.0

## FIGURES

FIG. 1. Total cross section for *a)*  $\widetilde{W}_1\widetilde{Z}_1$ , *b)*  $\widetilde{W}_1\widetilde{Z}_2$ , *c)*  $\widetilde{W}_1\widetilde{\overline{W}}_1$  and *d)*  $\widetilde{Z}_2\widetilde{Z}_2$  production in  $pp$  collisions at  $\sqrt{s} = 14$  TeV. Curves are for  $(m_{\widetilde{q}}/m_{\widetilde{g}}, \tan\beta) = (1,2)$  (solid),  $(1,20)$  (dashes), and  $(2,2)$  (dots). We have taken  $\mu = -m_{\widetilde{g}}$ .

FIG. 2. Selected branching fractions for  $\widetilde{W}_1$  decay versus  $m_{\widetilde{g}}$ , for *a)*  $(m_{\widetilde{q}}/m_{\widetilde{g}}, \tan\beta) = (1,2)$ , *b)*  $(1,20)$ , and *c)*  $(2,2)$ . We have taken  $\mu = -m_{\widetilde{g}}$ . The dashed curve is for  $\widetilde{W}_1 \rightarrow \mu\nu_\mu\widetilde{Z}_1$ , while solid is for  $\widetilde{W}_1 \rightarrow \widetilde{Z}_1W$ .

FIG. 3. Selected branching fractions for  $\widetilde{Z}_2$  decay versus  $m_{\widetilde{g}}$ , for *a)*  $(m_{\widetilde{q}}/m_{\widetilde{g}}, \tan\beta) = (1,2)$ , *b)*  $(1,20)$ , and *c)*  $(2,2)$ . We have taken  $\mu = -m_{\widetilde{g}}$ . The dashed curve is for  $\widetilde{Z}_2 \rightarrow \mu\bar{\mu}\widetilde{Z}_1$ , while solid is for  $\widetilde{Z}_2 \rightarrow \widetilde{Z}_1H_\ell$ , and dotted is for  $\widetilde{Z}_2 \rightarrow \widetilde{Z}_1Z$ .

FIG. 4. Distribution in missing transverse energy ( $\cancel{E}_T$ ) at LHC from *a)* all chargino-neutralino events and *b)* all other supersymmetric sources, after requiring three isolated leptons. We have illustrated spectra for text cases 1, 2 and 3 corresponding to  $m_{\widetilde{g}} = 300, 400$  and  $500$  GeV.

FIG. 5. Total cross section for trilepton signal after all cuts in the text, versus  $m_{\widetilde{g}}$ , for *a)*  $(m_{\widetilde{q}}/m_{\widetilde{g}}, \tan\beta) = (1,2)$ , *b)*  $(2,2)$ , *c)*  $(1,20)$  and *d)*  $(2,20)$ . We plot for  $\mu = -m_{\widetilde{g}}$  (x's) and  $\mu = +m_{\widetilde{g}}$  (o's). The dotted line corresponds to the SM background expected of  $WZ$  and  $t\bar{t}(135)$  while the dashed line denotes the same background for  $m_t = 175$  GeV.

FIG. 6. Distribution in OS dilepton invariant mass from both SUSY and SM sources (for  $m_t = 175$  GeV) after all cuts given in the text, for *a)* case 1, *b)* case 2 and *c)* case 3, corresponding to  $m_{\widetilde{g}} = 300, 400$  and  $500$  GeV. For  $\ell\ell'\bar{\ell}'$  events, we plot the mass of the same-flavor pair, while for  $\ell\ell\bar{\ell}$ , we plot the mass of the OS pair with smallest transverse opening angle.

FIG. 7. Distribution in trilepton plus  $\cancel{E}_T$  cluster transverse mass from both SUSY and SM sources after all cuts given in the text, for *a)* case 1, *b)* case 2 and *c)* case 3, corresponding to  $m_{\widetilde{g}} = 300, 400$  and  $500$  GeV (solid histogram). The dashed histograms are for corresponding distributions after setting  $m_{\widetilde{Z}_1} = 0$  by hand.

$(m_{\tilde{q}} / m_{\tilde{g}}, \tan \beta)$ : (1,2) = solid, (1,20) = dashes, (2,2) = dots

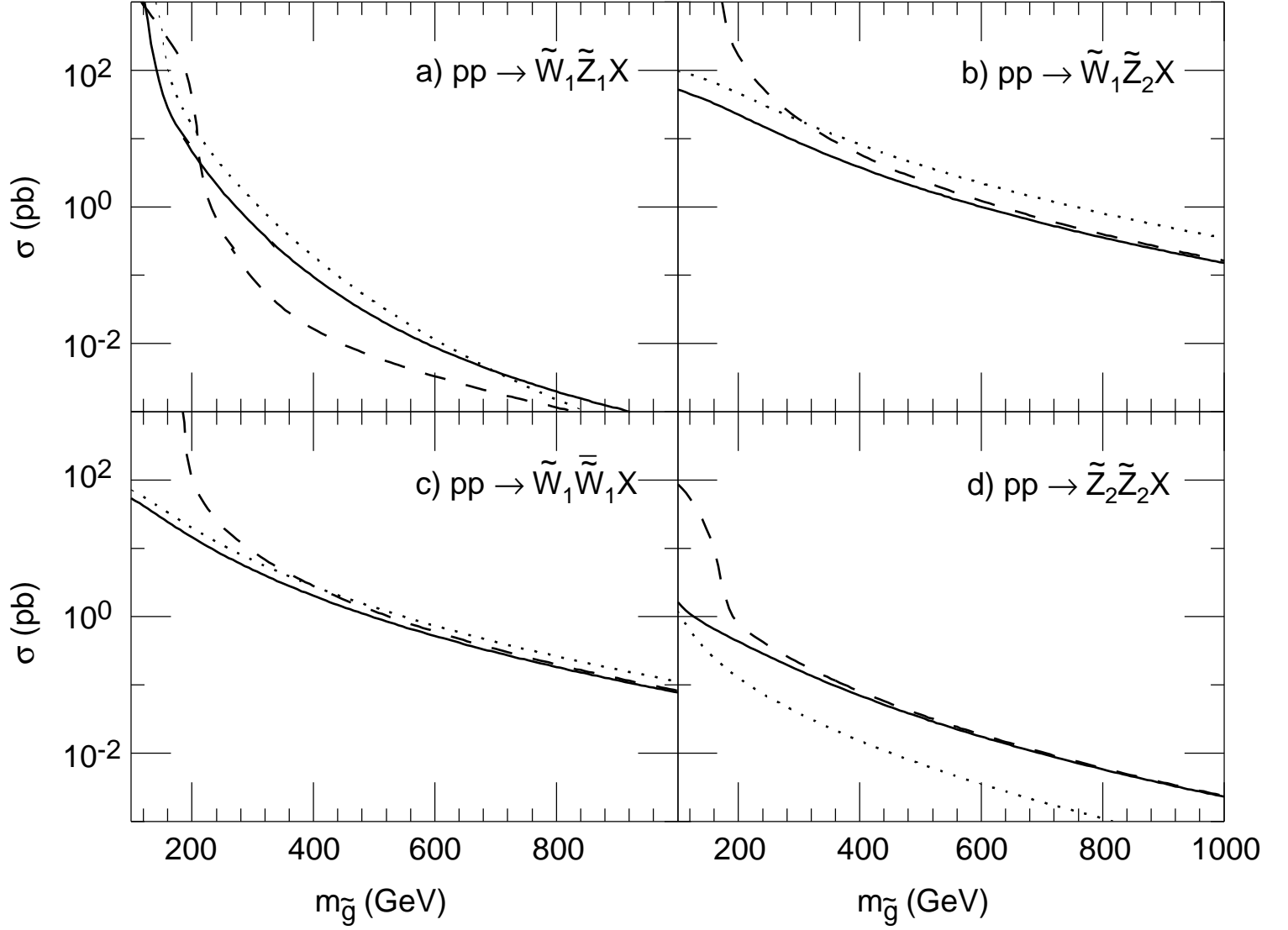


FIG. 1

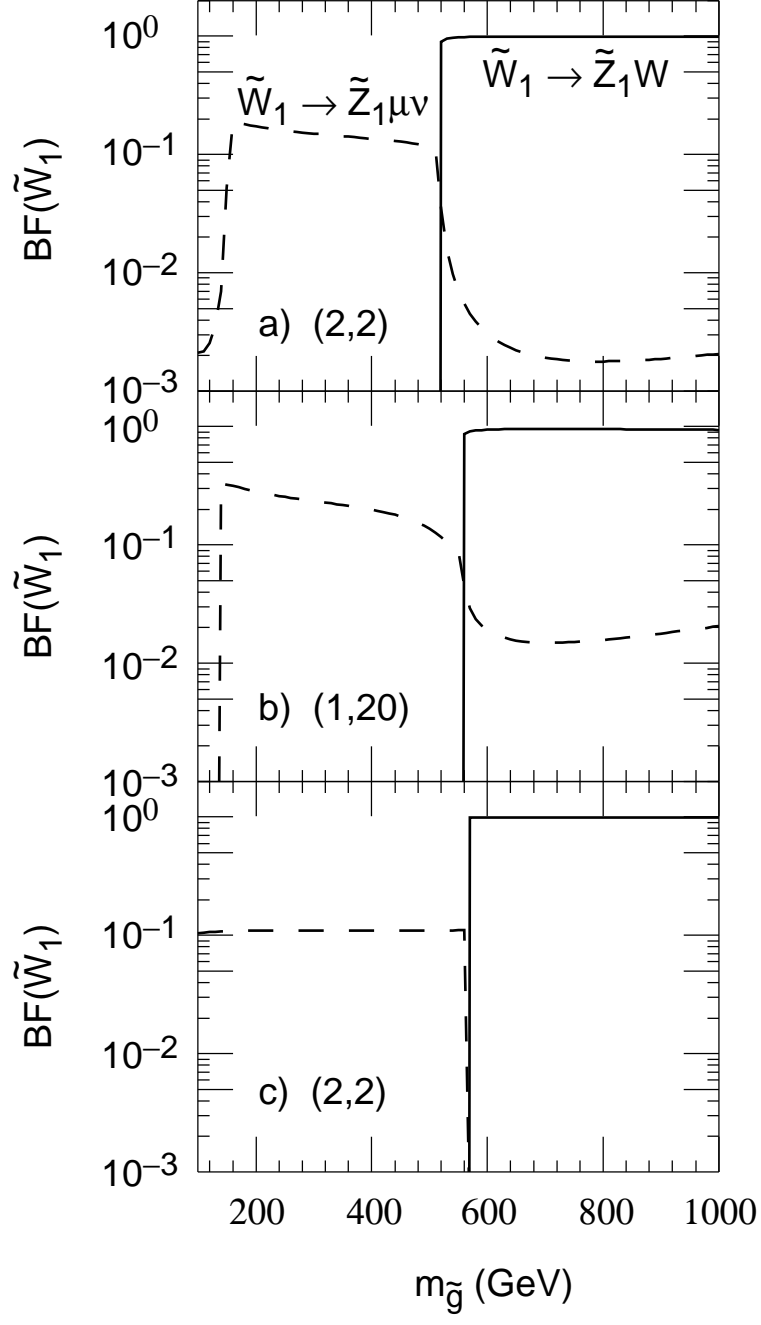


FIG. 2

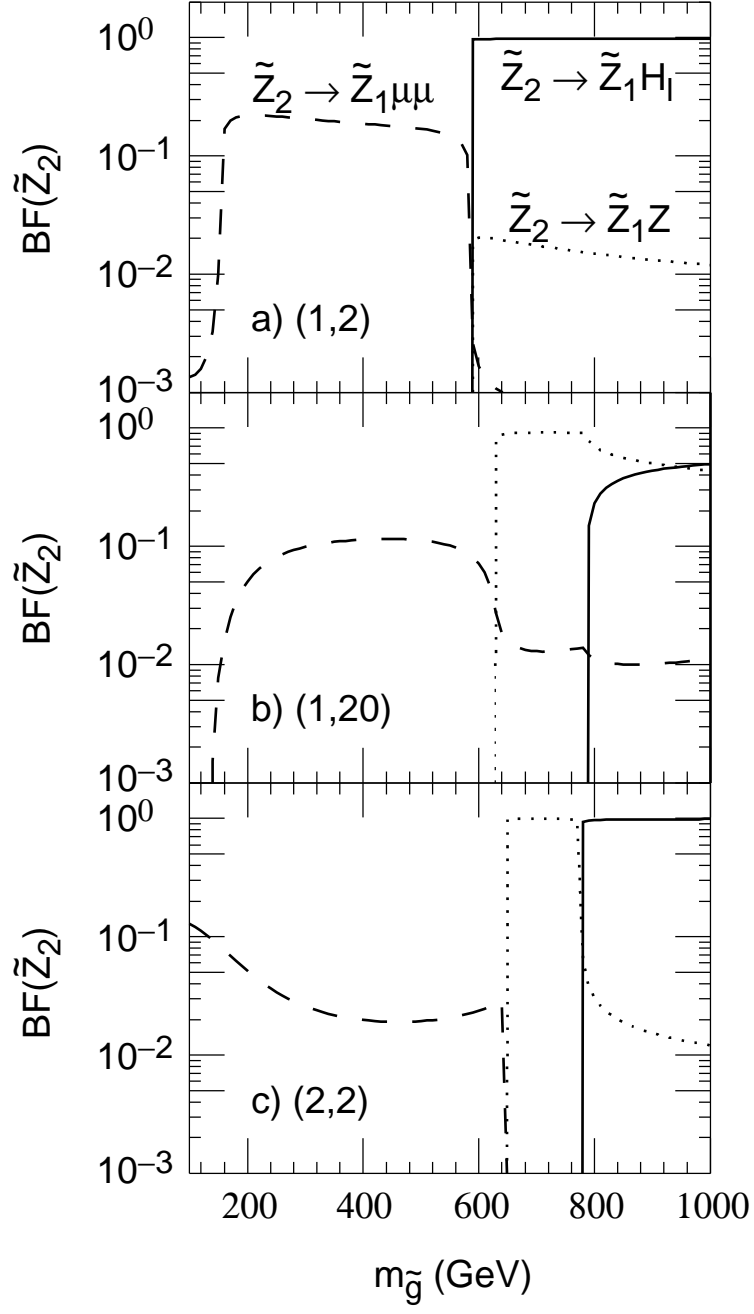


FIG. 3



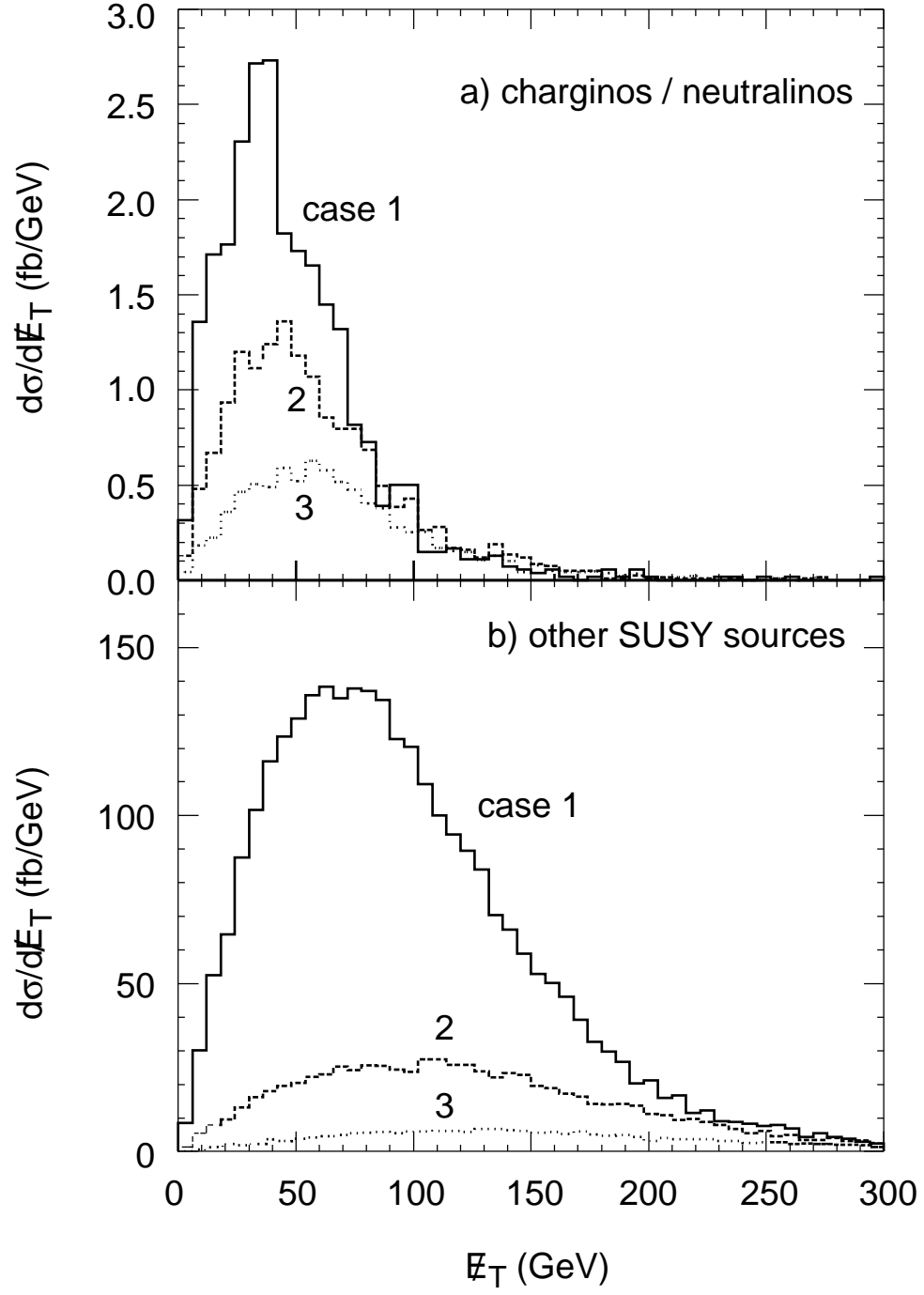


FIG. 4

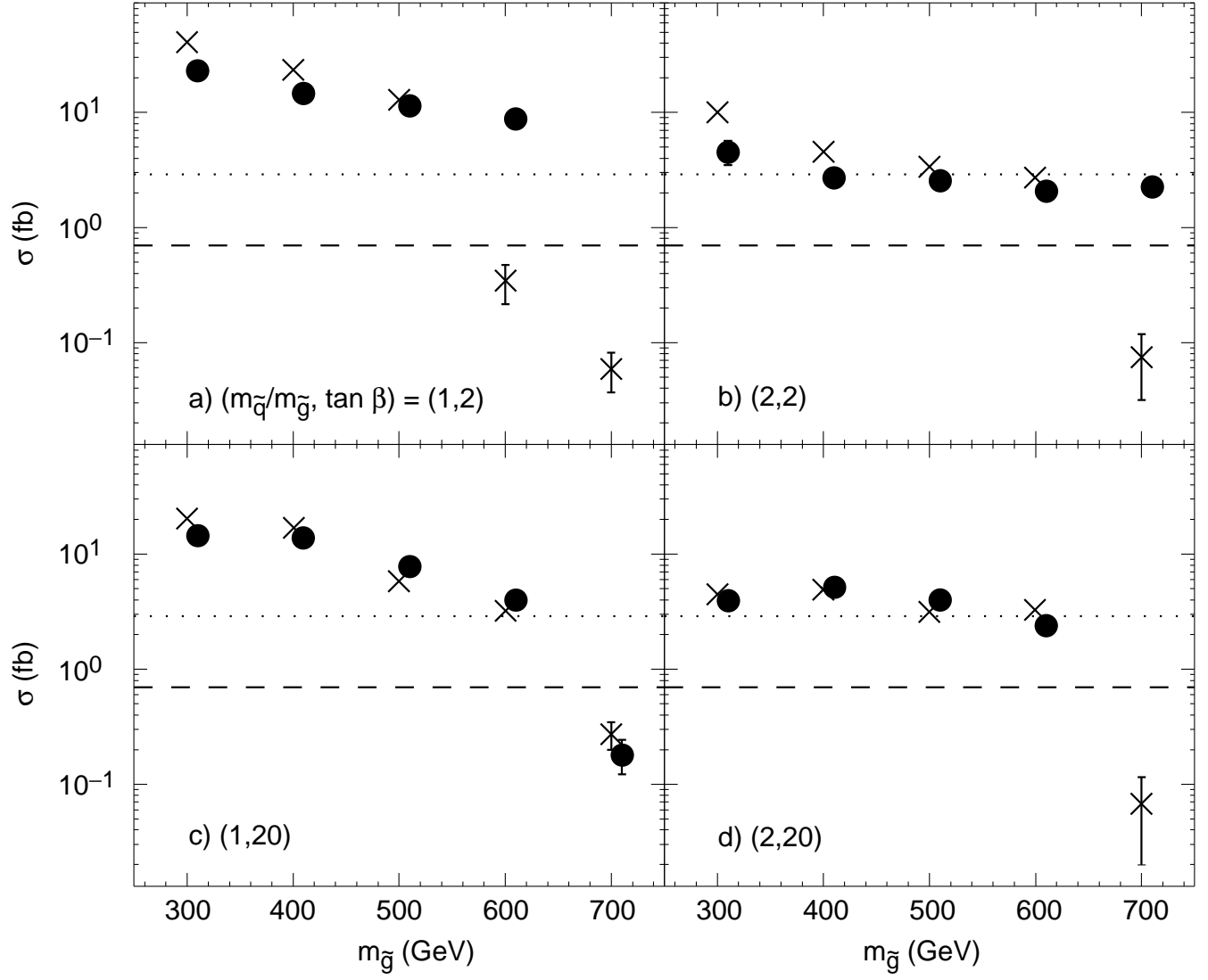


FIG. 5

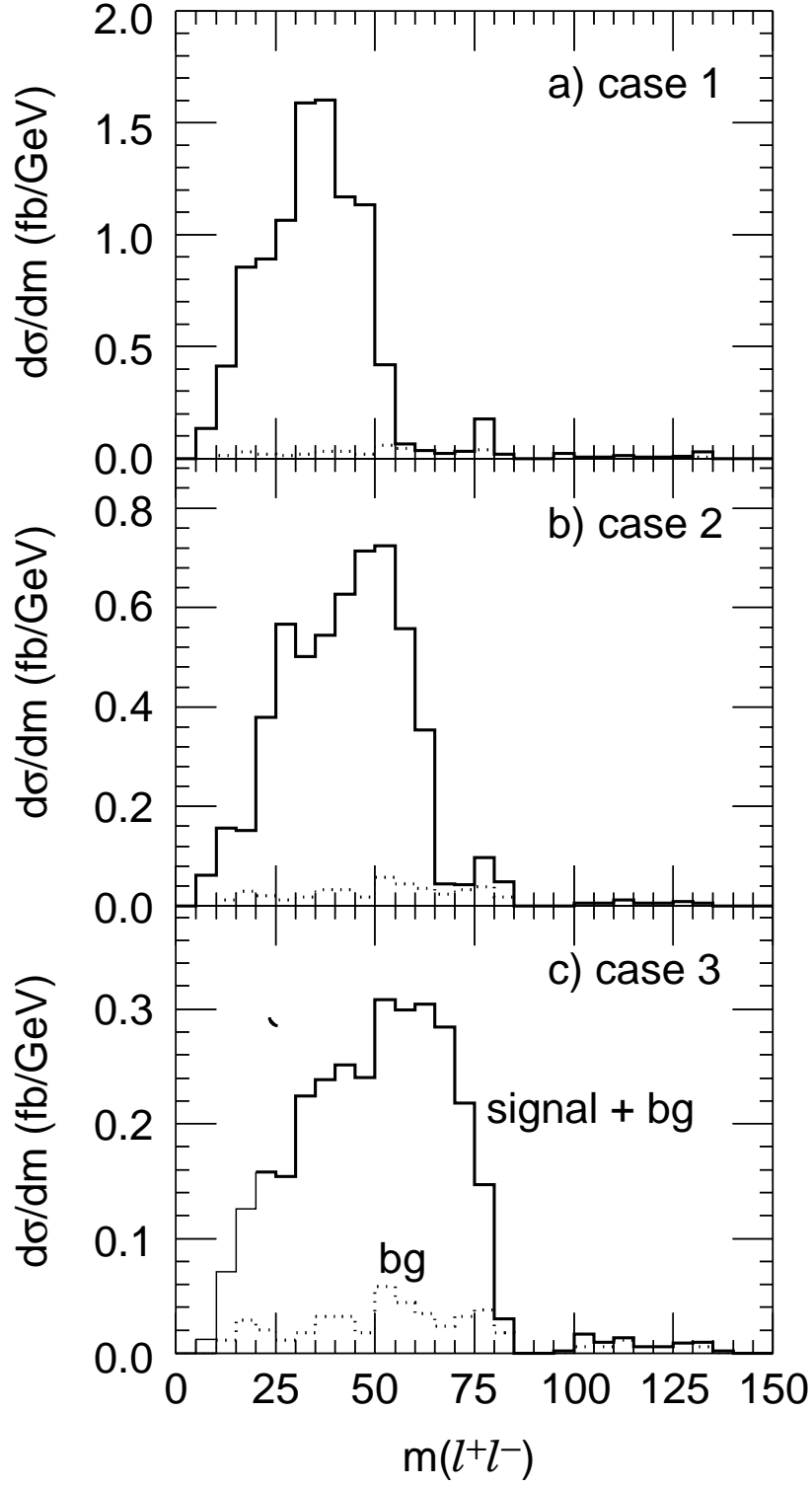


FIG. 6

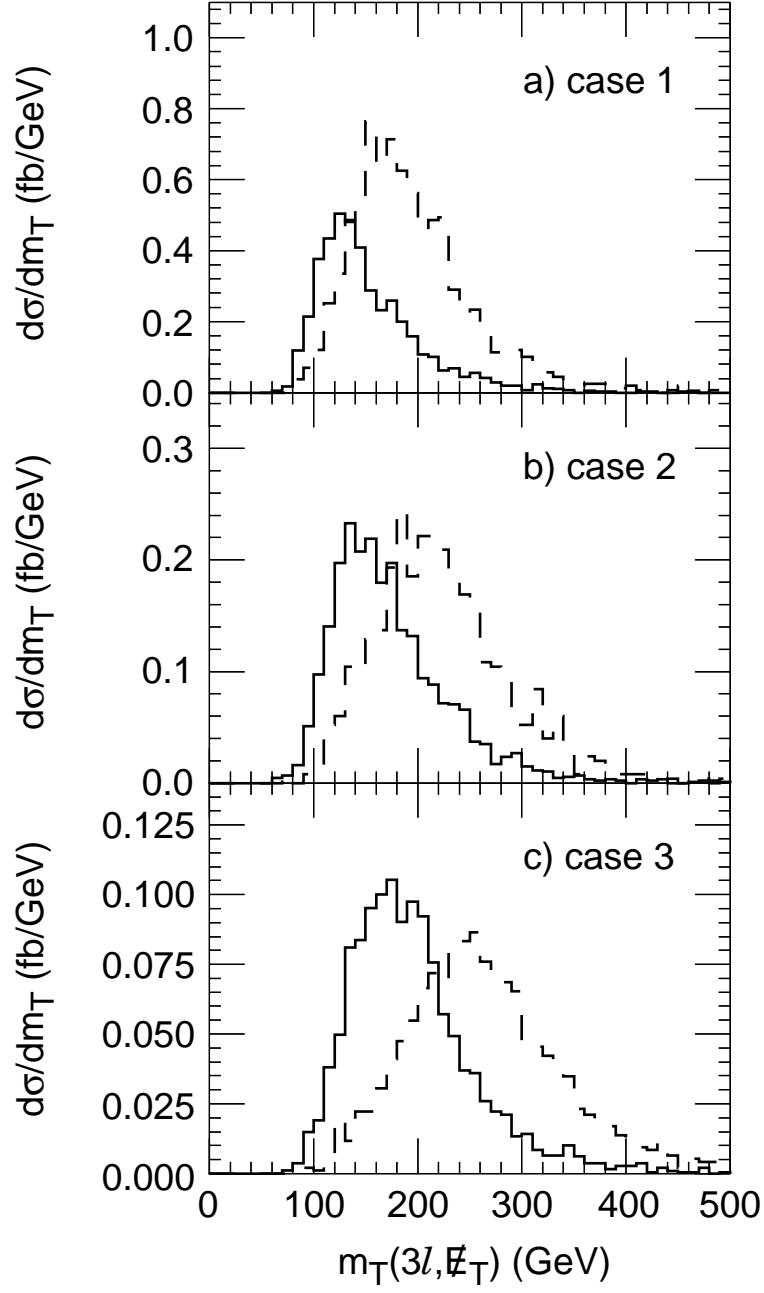


FIG. 7